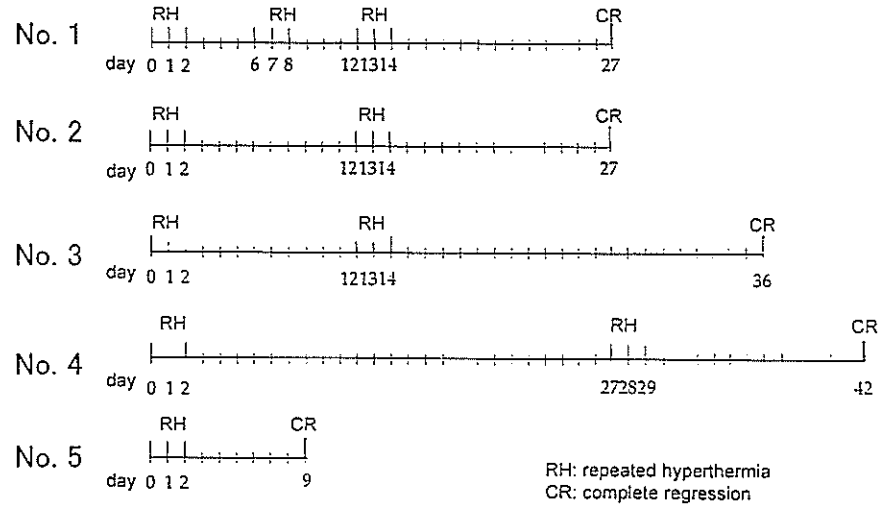

Fig. 7. Scheme of the hyperthermia experiment for the LNCap group, indicating the various patterns of RH among the five mice. The RH was repeated two or three times.

new hyperthermic procedure, we applied it whether RH could induce the CR of human prostate cancer cell lines (PC-3 and LNCap) in nude mice models. CR was induced in all the tumors in the PC-3 and LNCap groups (Figs. 6 and 8).

PC-3 is a cell line derived from bone metastatic lesions and is androgen-independent [28], whereas LNCap is derived from lymph node metastasic lesions and is androgen-sensitive [29]. In other words, these two prostatic cancer cell lines have different biological characters. In this study, our new hyperthermia method produced CR in all of the tumor nodules in the PC-3 and LNCap groups, although the rates of disappearance differed. In the LNCap group, linear involution started after just one round of RH, with CR occurring after one to three rounds of RH (Figs. 7 and 8). The PC-3 cancer nodules exhibited greater resistance to hyperthermia. In many cases of the PC-3 group, hyperthermia had no effect on tumor nodules during the first and second rounds, with the last tumors starting involution and exhibiting sudden CR after several RH rounds. This resulted in the total amount of RH rounds being greater for the PC-3 group than for the LNCap group (Figs. 5 and 6). The differing hyperthermic effects between PC-3 and LNCap can be explained as follows: when cultured at 43°C, the PC-3 cell population decreased according to cell-growth inhibition, whereas the LNCap cell population decreased according to a cell-killing effect. This difference is attributable to PC-3 cells possessing heat resistance in which hyperthermic stimulation stops the cell cycle, whereas LNCap cells are more sensitive to hyperthermia because the cell cycle does not change [30]. The huge variation in the time until CR (15–60 days in PC-3, 7–42 days in LNCap: Figs. 6 and 8) can be explained as follows: The distribution of magnetite nanoparticles within tumors must be considered in our use of a hyperthermia system to heat MCLs. When the MCLs were heated, the surrounding tumor tissues underwent necrosis, and magnetite nanoparticles subsequently expanded into the necrotic area within the tumor, resulting in a wide distribution of magnetite nanoparticles [21–23]. In the present study, CR of human prostate cancer cell nodules in nude mice was observed using a hyperthermia protocol, which should in fact be termed frequent RH. For LNCap in mouse 5, it took five rounds of RH to achieve CR. Although parts of the tumor containing sufficient amounts of MCLs were killed by heat, other parts of the tumor without MCLs—

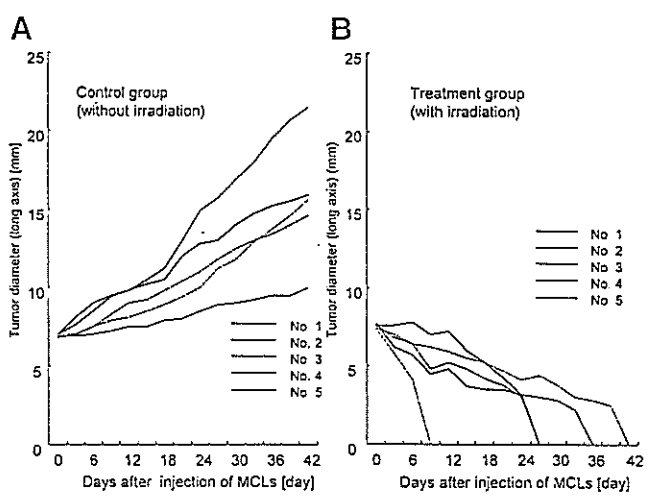

Fig. 8. Tumor long axis of the LNCap group in both the control group (A) and the treatment group (B). Tumor size increased linearly in the control group. However, a linear decrease and CR were demonstrated in the treatment group.

particularly at the tumor edges—may continue to grow. Therefore, differences in the number of rounds of RH treatment for CR are probably due to variations in the tumor shape.

It is well known that there is no reliable therapy for hormone-refractory prostate cancer [31,32]. The use of frequent RH in the present study resulted in CR of PC-3 tumor nodule, which are androgen-independent. This result suggests that frequent RH could be used as one of treatment for hormone-refractory prostate cancer. Since our new hyperthermia technique can induce CR in cancer tissue only by heating, it may be a useful therapy in various types of cancer. From the perspective point of view for clinical use, our new MCL-induced hyperthermia technique will be especially useful if irradiation with an AMF in the FCIS can adequately increase the temperature of tumor tissue injected with MCLs positioned 50 mm above the surface of the coil. The major tumor mass is peripheral in location in clinical stage T2 carcinomas and in 85% of nonpalpable tumors diagnosed on needle biopsy (stage T1c) [33–35], and can be heated by an FCIS attached to the perineal portion since the magnetic flux reaches the peripheral zone of the prostate. In the remaining cases, tumors are predominatly located in the transition zone, and adenocarcinoma of the prostate is multifocal in more than 85% of cases [34]. The development of an endoscopic AMF-generation machine would enable tumors in the transition zone and other multifocal tumors to be treated. The further development of the FCIS will allow our new MCL-induced hyperthermia technique to become a new treatment method for hormone-refractory prostate cancer.

ACKNOWLEDGMENTS

This work was partially supported by a Grant-in-Aid for Scientific Research (No. 13853005), University Start-Ups Creation Support System, and the 21st Century COE Program "Nature-Guided Materials Processing" from the Ministry of Education, Culture, Sports, Science, and Technology of Japan.

REFERENCES

1. Levi F, Lucchini F, Negri E, Boyle P, La Vecchia C. Changed trends of cancer mortality in the elderly. Ann Oncol 2001;12: 1467–1477.
2. Littrup PJ. Future benefits and cost-effectiveness of prostate carcinoma screening. American Cancer Society. Cancer 1997;80:1864–1870.
3. Smart CR. The results of prostate carcinoma screening in the U.S. as reflected in the surveillance, epidemiology, and end results program. Cancer 1997;80:1835–1844.
4. Schellhammer PF. Editorial: Improving outcomes for primary and salvage therapy of localized prostate cancer. J Urol 2003; 170:1841–1842.
5. Akaza H, Homma Y, Okada K, Yokoyama M, Moriyama N, Usami M, Hirao Y, Tsushima T, Ohashi Y, Aso Y. Early results of LH-RH agonist treatment with or without chlormadinone acetate for hormone therapy of naive localized or locally advanced prostate cancer: A prospective and randomized study. The Prostate Cancer Study Group. Jpn J Clin Oncol 2000;30:131–136.
6. Han KR, Cohen JK, Miller RJ, Pantuck AJ, Freitas DG, Cuevas CA, Kim HL, Lugg J, Childs SJ, Shuman B, Jayson MA, Shore ND, Moore Y, Zisman A, Lee JY, Ugarte R, Mynderse LA, Wilson TM, Sweat SD, Zinck eH, Belldegrun AS. Treatment of organ confined prostate cancer with third generation cryosurgery: Preliminary multicenter experience. J Urol 2003;170:1126–1130.
7. Chin JL, Touma N, Pautler SE, Guram KS, Bella AJ, Downey DB, Moussa M. Serial histopathology results of salvage cryoablation for prostate cancer after radiation failure. J Urol 2003;170:1199–1202.
8. Johnson DB, Nakada SY. Cryoablation of renal and prostate tumors. J Endourol 2003;17:627–632.
9. Rouviere O, Lyonnet D, Radiant A, Colin-Pan gaud C, Chapelon JY, Bouvier R. Dubernard JM, Gelet A. MRI appearance of prostate following transrectal HIFU ablation of localized cancer. Eur Urol 2001;40:265–274.
10. Gelet A, Chapelon JY, Bouvier R, Pangaud C, Lasne Y. Local control of prostate cancer by transrectal high intensity focused ultrasound therapy: Preliminary results. J Urol 1999;161: 156–162.
11. Van Leenders GJ, Beerlage HP, Ruijter ET, de la Rosette JJ, van de Kaa CA. Histopathological changes associated with high intensity focused ultrasound (HIFU) treatment for localised adenocarcinoma of the prostate. J Clin Pathol 2000;53:391–394.
12. Van der Zee J. Heating the patient: A promising approach? Ann Oncol 2002;13:1173–1184.
13. Abe M, Hiraoka M, Takahashi M, Egawa S, Matsuda C, Onoyama Y, Morita K, Kakehi M, Sugahara T. Multi-institutional studies on hyperthermia using an 8-MHz radiofrequency capacitive heating device (Thermotron RF-8) in combination with radiation for cancer therapy. Cancer 1986;58:1589–1595.
14. Kroeze H, van de Kamer JB, de Leeuw AA, Kikuchi M, Lagendijk JJ. Treatment planning for capacitive regional hyperthermia. Int J Hyperthermia 2003;19:58–73.
15. Sherar MD, Gertner MR, Yue CK, O'Malley ME, Toi A, Gladman AS, Davidson SR, Trachtenberg J. Interstitial microwave thermal therapy for prostate cancer: Method of treatment and results of a phase I/II trial. J Urol 2001;166:1707–1714.
16. Tucker RD, Huidobro C, Larson T, Platz CE. Use of permanent interstitial temperature self-regulating rods for ablation of prostate cancer. J Endourol 2000;14:511–517.
17. Master VA, Shinohara K, Carroll PR. Ferromagnetic thermal ablation of locally recurrent prostate cancer: Prostate specific antigen results and immediate/intermediate morbidities. J Urol 2004;172:2197–2202.
18. Deger S, Taymoorian K, Boehmer D, Schink T, Roigas J, Wille AH, Budach V, Wernecke KD, Loening SA. Thermoradiotherapy using interstitial self-regulating thermoseeds: An intermediate analysis of a phase II trial. Eur Urol 2004;45:574–579.
19. Moroz P, Jones SK, Gray BN. Magnetically mediated hyperthermia: Current status and future directions. Int J Hyperthermia 2002;18:267–284.

20. Shinkai M, Yanase M, Honda H, Wakabayashi T, Yoshida J, Kobayashi T. Intracellular hyperthermia for cancer using magnetite cationic liposomes: In vitro study. Jpn J Cancer Res 1996;87:1179–1183.
21. Yanase M, Shinkai M, Honda H, Wakabayashi T, Yoshida J, Kobayashi T. Intracellular hyperthermia for cancer using magnetite cationic liposomes: Ex vivo study. Jpn J Cancer Res 1997;88:630–632.
22. Yanase M, Shinkai M, Honda H, Wakabayashi T, Yoshida J, Kobayashi T. Intracellular hyperthermia for cancer using magnetite cationic liposomes: An in vivo study. Jpn J Cancer Res 1998;89:463–469.
23. Yanase M, Shinkai M, Honda H, Wakabayashi T, Yoshida J, Kobayashi T. Antitumor immunity induction by intracellular hyperthermia using magnetite cationic liposomes. Jpn J Cancer Res 1998;89:775–782.
24. Kawai N, Ito A, Nakahara Y, Futakuchi M, Shirai T, Honda H, Kobayashi T, Kohri K. Anticancer effect of hyperthermia on prostate cancer mediated by magnetite cationic liposomes and immune-response induction in transplanted syngeneic rats. Prostate 2005;64:373–381.
25. Shinkai M, Ueda K, Ohtsu S, Honda H, Kobayashi T. Effect of functional magnetid particles on frequency capative heating. Japanese Journal of Cancer Research 1999; 90:699–704.
26. Cetas TC, Gross EJ, Contractor Y. A ferrite core/metallic sheath thermoseed for interstitial thermal therapies. IEEE Transactions on Biomedical Engineering 1998;45:68–77.
27. Ito A, Tanaka K, Honda H, Abe S, Yamaguchi H, Kobayashi T. Complete regression of mouse mammary carcinoma with a size greater than 15 mm by frequent repeated hyperthermia using magnetite nanoparticles. J Biosciences and Bioengneering 2003; 4:364–369.
28. Kaighn ME, Narayan KS, Ohnuki Y, Lechner JF, Jones LW. Establishment and characterization of a human prostatic carcinoma cell line (PC-3). Invest Urol 1979;17:16–23.
29. Horoszewicz JS, Leong SS, Kawinski E, Karr JP, Rosenthal H, Chu TM, Mirand EA, Murphy GP. LNCaP model of human prostatic carcinoma. Cancer Res 1983;43:1809–1818.
30. Nakanoma T, Ueno M, Iida M, Hirata R, Deguchi N. Effects of quercetin on the heat-induced cytotoxicity of prostate cancer cells. Human cell 2001;11:623–630.
31. Kasamon KM, Dawson NA. Update on hormone-refractory prostate cancer. Curr Opin Urol 2004;14:185–193.
32. Deutsch E, Maggiorella L, Eschwege P, Bourhis J, Soria JC, Abdulkarim B. Environmental, genetic, and molecular features of prostate cancer. Lancet Oncol 2004;5:303–313.
33. McNeal JE. Origin and development of carcinoma in the prostate. Cancer 1969;23:24–34.
34. Byar DP, Mostofi FK. Carcinoma of the prostate: Prognostic evaluation of certain pathologic features in 208 radical prostatectomies. Examined by the step-section technique. Cancer 1972; 30:5–13.
35. Epstein JI, Walsh PC, Carmichael M, Brendler CB. Pathologic and clinical findings to predict tumor extent of non palpable (stage T1c) prostate cancer. JAMA 1994;271:368–374.

Inhibition of prostate carcinogenesis in probasin/SV40 T antigen transgenic rats by leuprorelin, a luteinizing hormone–releasing hormone agonist

Mahmoud M. Said,[1,2] Naomi Hokaiwado,[1] Mingxi Tang,[1] Kumiko Ogawa,[1] Shugo Suzuki,[1] Hala M. Ghanem,[2] Amr Y. Esmat,[2] Makoto Asamoto,[1] Fawzia M. Refaie[2] and Tomoyuki Shirai[1,3]

[1]Department of Experimental Pathology and Tumor Biology, Nagoya City University Graduate School of Medical Sciences, Nagoya, 467-8601, Japan; and [2]Department of Biochemistry, Faculty of Science, Ain Shams University, Cairo, Egypt

(Received November 28, 2005/Revised January 23, 2006/Accepted February 16, 2006/Online publication May 11, 2006)

The effects of leuprorelin acetate, a luteinizing hormone-releasing hormone agonist (LHRH-A), on prostate carcinogenesis in probasin/SV40 Tag transgenic rat was investigated. Fifteen weeks after administration of 0.28 and 2.8 mg/kg leuprorelin, prostate weights and serum testosterone levels were significantly decreased compared to values for transgenic controls. Histopathological findings revealed that the incidence of prostatic adenocarcinomas was significantly reduced in ventral, dorsal and lateral lobes of the prostate, correlating with decreased expression of SV40 Tag oncoprotein as well as inhibition of DNA synthesis and proliferation of epithelial cells in neoplastic lesions of the ventral prostate. Microarray analysis further showed leuprorelin acetate to significantly inhibit testicular steroidogenesis, suppressing the expression of SV40 Tag oncoprotein and altering the expression of a large number of genes which might be involved in the inhibition of prostate cancer progression in this rat model. (*Cancer Sci* 2006; 97: 459–467)

Prostate cancer has become the most commonly diagnosed malignancy in men, and the second commonest cause of cancer death after lung neoplasms in the USA.[1] Initial treatment of prostate cancer is usually androgen-ablative therapy, radiotherapy or radical prostatectomy, and patients with early stage disease respond well. However, in many patients the therapy eventually fails and death occurs from recurrent androgen-independent prostate cancer and metastasis.

Luteinizing hormone-releasing hormone (LHRH), which is synthesized in hypothalamic neurons and secreted directly into the hypophyseal-portal blood circulation in a pulsatile manner, binds to high-affinity receptors (LHRH-R) on the gonadotrophic cells in the pituitary, stimulating the synthesis and release of luteinizing hormone (LH) and follicle-stimulating hormone (FSH), which in turn stimulate the synthesis of sex steroids by the testes. Based on the hypothalamus-pituitary-gonad hormonal relationship, LHRH analogs have been developed and used to treat prostate cancer through suppression of the pituitary release of gonadotropins to achieve a chemical castration effect. The mechanism of action is presumed to result from desensitization or downregulation of LHRH receptors in the pituitary gonadotrophs after chronic exposure to LHRH agonists and a consequent decline of gonadotropin secretion and subsequent gonadal atrophy.[2,3] However, the molecular mechanisms involved in the inhibition of prostatic carcinomas by LHRH agonists are poorly defined.

Various studies have demonstrated that LHRH analogs inhibit the proliferation of human prostate cancer cell lines and prostate cancer xenografts, and also reduce the growth of androgen-dependent and independent rat Dunning tumors, suggesting that their effects are mediated by specific LHRH receptors. This has been confirmed by detection of LHRH receptor mRNA expression in human prostate cancer cell lines and prostate cancer tissues. Therefore, activation of LHRH receptors at the prostate tumor level may represent an additional and more direct mechanism of action for antitumoral LHRH agonists.[4,5]

Leuprorelin acetate is a highly superactive agonistic analog of LHRH which is reported to inhibit pituitary gonadotropin secretion and suppress testicular steroidogenesis when administered chronically in therapeutic doses.[6,7] Leuprorelin treatment is an established effective palliative measure in men with previously untreated advanced prostatic cancer, and is therefore a reasonable non-surgical alternative in patients with prostatic disorders associated with aging.[8]

A rat transgenic model producing well-differentiated prostate adenocarcinomas in all prostatic lobes and in a short period (15 weeks of age) using the Simian virus 40 T antigen under control of the probasin gene promoter (PB/SV40 Tag) has been established in our laboratory.[9] This rat model of prostate carcinogenesis, which is completely androgen-dependent, provides a good tool to evaluate strategies for prevention and treatment of prostate cancer in a relatively short-term.

The present study was undertaken to investigate the effects of leuprorelin acetate on prostate carcinogenesis using our PB/SV40 Tag transgenic rats, with special attention to molecular changes in response to leuprorelin treatment, assessed by microarray analysis.

Materials and Methods

Animals

Heterozygous probasin-SV40 large T antigen (PB/SV40 Tag) transgenic male rats for this study were obtained by mating

[3]To whom correspondence should be addressed.
E-mail: tshirai@med.nagoya-cu.ac.jp

doi: 10.1111/j.1349-7006.2006.00213.x

heterologous transgenic males and wild-type Sprague Dawley female rats (Clea, Tokyo, Japan). Rats weighing 110–150 g and aged 5 weeks at the commencement were used. They were ear-tagged and housed three rats per plastic cage on wood-chip bedding in an air-conditioned specific pathogen-free (SPF) animal room at 22 ± 2°C and 55 ± 5% humidity with a 12 h light/dark cycle. The animals had free access to food (Oriental MF, Oriental Yeast, Tokyo, Japan) and water. All animal experiments were performed under protocols approved by the Institutional Animal Care and Use Committee of Nagoya City University School of Medicine.

Screening of transgenic rats

DNA samples were obtained from rat tails by the proteinase K/phenol/chloroform method. Polymerase chain reaction (PCR) was performed using Taq polymerase (TaKaRa, Japan) to amplify a 300 bp fragment of SV40 Tag. Primers used were 5′-AGCCCTGTCCTCCTGCAGGAT-3′ (upper primer) and 5′-GGCCAGCCTCACGGGGTTCA-3′ (lower primer) (Hokkaido System Science, Japan).

Chemicals

Leuprorelin acetate (Leuplin) was kindly donated by Takeda Chemical Industries (Osaka, Japan) in a white powder form as a microcapsule sustained-release preparation (microspheres of 20 μm diameter). The molecular weight is 1269.47 and the chemical comprises nine amino acids and has the empiric formula of $C_{59}H_{84}N_{16}O_{12}.C_2H_4O_2$.[10]

Stock leuprorelin solution (1.875 mg/mL) was freshly prepared by suspending a vial of leuprorelin (3.75 mg leuprorelin acetate, 33.1 mg DL-lactic and glycolic acids copolymer [3:1], 0.65 mg purified gelatin and 6.6 mg D-mannitol) into 2 mL of diluent (100 mg D-mannitol, 10 mg sodium carboxymethyl cellulose and 2 mg polysorbate-80) from which two doses (high-dose; 2.8 mg/kg and low-dose; 0.28 mg/kg) were prepared and subcutaneously administered to the back of rats once every 4 weeks for a total of four injections.[11]

Study design

A total of 36 heterozygous transgenic male rats were allocated into four equally sized groups so that there were no significant differences in mean bodyweights. Group I (controls) comprised transgenic rats with the probasin/SV40 Tag serving as the reference group. Group II (vehicle) comprised PB/SV40 Tag transgenic animals which received a subcutaneous injection of the diluent (1.5 mL/kg) once every 4 weeks for a total of four injections. Group III (low-dose) comprised transgenic animals that received a subcutaneous injection of leuprorelin at 0.28 mg/kg once every 4 weeks for a total of four injections. Group IV (high-dose) comprised transgenic animals which received a subcutaneous injection of leuprorelin at 2.8 mg/kg once every 4 weeks for a total of four injections. Animal weights were recorded weekly throughout the experimental period (15 weeks).

Blood collection and tissue sampling

At the end of the treatment period (15 weeks), animals in all groups were intraperitoneally injected 1 h before being killed with 2% 5-bromo-2′-deoxyuridine solution (BrdU) at a dose of 100 mg/kg bodyweight.[12] Blood was collected from the abdominal aorta under ether anesthesia into 10 mL plastic vacuum tubes, kept on ice to clot and centrifuged. Serum samples were then analyzed for total testosterone with a direct radioimmunoassay (RIA) kit (Diagnostic Products Corporation, USA), for LH and FSH with double antibody RIA research kits (Amersham Biosciences, UK), and for urea nitrogen and creatinine levels using commercial kits (Alfresa Pharma, Japan). The urinogenital organs, comprising the prostate gland, seminal vesicles and urinary bladder were excised, weighed and photographed. Both ventral prostate lobes were separated and weighed. One lobe together with the pituitary gland was immediately frozen in liquid nitrogen then stored at −80°C until RNA extraction, while the other lobe together with the remaining prostates and tongues was fixed in 10% phosphate-buffered formalin for 48 h, routinely processed to hematoxylin and eosin (HE) stained sections and histopathologically examined. Livers, kidneys and testes were excised at necropsy and weighed.

Immunohistochemistry

Immunohistochemical analyses of androgen receptor (AR) and SV40 Tag expression were performed with a Discovery instrument using DAB Map kits (Ventana Medical Systems, USA) with polyclonal rabbit antiandrogen receptor (PA1-110, Affinity BioReagents, USA) and monoclonal mouse anti-SV40 large T antigen (554149, BD PharMingen, USA) antibodies. Binding was visualized with a Vectastain Elite ABC kit (Vector Laboratories, USA) and light hematoxylin counterstaining was conducted to facilitate microscopic examination. Furthermore, the effects of administration of leuprorelin acetate on DNA synthesis in the epithelial cells of the ventral prostates of PB/SV40 Tag transgenic rats was investigated using BrdU immunostaining using a monoclonal mouse antibromodeoxyuridine antibody (Dako, Denmark). The numbers of BrdU positive cells were counted in 1000 cells/slide and BrdU labeling indices was determined with the following equation: (number of labeled cells/number of total cells) × 100.

Extraction of RNA

Extraction of total RNA from rat ventral prostate lobes as well as pituitary glands for reverse transcription (RT)-PCR and microarray analyses was performed according to an ISOGEN protocol (Nippon Gene, Japan) with DNase treatment using a RQ1 RNase-Free DNase kit (Promega Corporation, USA). Concentration and purity of total RNAs were assessed by measuring absorbance at 260 and 280 nm with a spectrophotometer (Ultrospec 3300 pro, Amersham Pharmacia Biotech, USA) and quality was assessed with an Agilent 2100 Bioanalyzer using a RNA 6000 Nano LabChip Kit (Agilent Technologies, USA). For microarray assays, the concentration, purity and quality of RNA should be >2, with an A_{260}:A_{280} between 1.8 and 2.1, and the 28S:18S ratio should approach 2. Extracted RNA samples were stored at −80°C.

Quantitative RT-PCR analyses of mRNA expression of SV40 Tag, androgen receptor and LHRH-receptors

One microgram of RNA was converted to cDNA with avian myeloblastosis virus (AMV) reverse transcriptase (TaKaRa, Japan) in a 20 μg reaction mixture. Aliquots of 2 μg of cDNA samples were subjected to quantitative RT-PCR using

doi: 10.1111/j.1349-7006.2006.00213.x

SYBR Premix ExTaq (TaKaRa) in a light cycler apparatus (Roche Diagnostic, Mannheim, Germany). Primers used for SV40 Tag were 5′-GTCAGCAGTAGCCTCATCAT-3′ and 5′-GGTTGATTGCTACTGCTTCG-3′; primers for AR were 5′-GACTATTACTTCCCACCCCAG-3′ and 5′-ACATTTCCGGAGACGACACGA-3′; primers for LHRH-R were 5′-CTTGAAGCCCGTCCTTGGAGAAAT-3′ and 5′-GCGATCCAGGCTAATCACCACCAT-3′; and primers for rat cyclophilin (housekeeping gene) were 5′-TGCTGGACCAAACACAAATG-3′ and 5′-GAAGGGGAATGAGGAAAATA-3′. The LightCycler amplification protocol consisted of four programs: program 1, preincubation and denaturation of the template DNA (one cycle; 95°C for 30 s); program 2, amplification of the target DNA (30–40 cycles of denaturation at 95°C for 5 s, primer annealing at 45°C for SV40 Tag, 52°C for AR, 55°C for cyclophilin and 60°C for LHRH-R for 15 s and elongation at 72°C for 30 s); program 3, melting curve analysis for product identification (95°C for 0 s, 65°C for 15 s and 95°C for 0 s); and program 4, cooling of the rotor and thermal chamber (one cycle; 40°C for 30 s). Cyclophilin mRNA levels were used to normalize sample cDNA contents.

Microarray analysis of gene expression profiles

Gene expression profiling was conducted using the CodeLink Expression Bioarray System (Amersham Biosciences, USA). The CodeLink Rat Whole Genome Bioarray targets ~34 000 transcripts and Expressed Sequence Tags (ESTs) including over 29 000 well substantiated rat genes along with probes for housekeeping genes for normalization as well as positive and negative bacterial controls.

Because both low and high doses of leuprorelin showed parallel inhibition of prostatic adenocarcinoma development, the low dose was chosen for gene expression profiling analysis compared to the controls.

One RNA sample with a final concentration of 2 μg (pooled from three animals/group) was prepared and used to probe a single microarray chip. Hybridizations were performed as directed by CodeLink instructions. Briefly, mRNA was hybridized with an oligo-dT primer that contained additional sequences corresponding to one strand of T7 RNA polymerase promoter. The oligo-dT-primed mRNA was converted to single-stranded cDNA with reverse transcriptase then into double-stranded cDNA with DNA polymerase. Double-stranded cDNA was captured using QIAquick columns (QIAGEN, Germany) and served as a template for *in vitro* transcription (IVT) by T7 RNA polymerase in the presence of biotin-UTP (PerkinElmer Life Sciences, USA) to produce biotin-labeled target cRNA transcripts that were collected on RNeasy columns (QIAGEN). Target cRNA was fragmented followed by overnight hybridization with the bioarray chip in a temperature-controlled shaking incubator. Spots were visualized using Cy5-streptavidin dye conjugate and bioarrays were scanned and hybridization intensities were analyzed with CodeLink Expression Analysis software (Amersham Biosciences). The expression ratio for each gene was calculated between leuprorelin-treated transgenic animals and controls. More than a two-fold increase or decrease was regarded as a significant change (>2 as upregulated and <0.5 as downregulated). Overexpressed and downregulated genes were then annotated and grouped by function using the public database SOURCE.

Statistical analysis

The statistical significance of the incidence of neoplastic lesions in the prostates was assessed by Scheffe's analysis. Statistical analysis of differences between means was carried out using analysis of variance (ANOVA). When significant differences were obtained between means, the post-hoc Bonferroni's test for multiple comparisons was used to evaluate the statistical significance between treatment groups at the $P < 0.05$ level of significance.

Results

Effects of leuprorelin treatment on body and organ weights in PB/SV40 Tag transgenic rats

Non-significant changes in total bodyweights were recorded in vehicle or leuprorelin treated animals throughout the experiment compared to controls, demonstrating subchronic administration (15 weeks) of leuprorelin to transgenic rats to be non-toxic.

Effects of leuprorelin treatment on the gross appearance of prostate and seminal vesicles

Macroscopically, prostates of the control and vehicle treated rats showed irregular surfaces with no apparent nodule or mass formation. Treatment of rats with low and high doses of leuprorelin markedly reduced the gross weights of the prostate and seminal vesicles in comparison to control and vehicle treated animals, without any apparent difference between the two dose groups (Fig. 1, Table 1).

Effects of leuprorelin treatment on serum LH, FSH and testosterone in PB/SV40 Tag transgenic rats

PB/SV40 Tag transgenic rats treated with low and high doses of leuprorelin for 15 weeks demonstrated a significant reduction in serum total testosterone level that reached 56.8% and 82.1%, respectively. No significant changes were observed in serum LH or FSH compared to controls.

Effects of leuprorelin treatment on the incidence of neoplastic lesions in the prostate

Prostate lesions in control rats showed marked epithelial proliferation with the formation of irregular glands and luminal bridging to give cribriform patterns. The nuclei demonstrated enlargement and severe atypia, and the lesions were compatible with human adenocarcinomas and were therefore diagnosed as such. Glands with less proliferation were also observed. These exhibited crowding of stratified epithelial cells with irregular spacing and occasional luminal bridging. Although nuclear atypia were severe, basic glandular structures were maintained, similar to normal prostates, and the lesions were diagnosed as prostatic intraepithelial neoplasia (PIN), comparable with the human lesions.[9]

Adenocarcinomas were composed of atypical cells with many mitoses forming glandular and cribriform structures. Histopathological examination revealed a 100% incidence of prostate adenocarcinomas in the ventral, lateral and anterior lobes at 20 weeks of age in the control and vehicle treated groups (Table 2), whereas the incidence was 55.6% and 66.7% in the dorsal prostate lobes, respectively. Low and high doses of leuprorelin significantly reduced the incidence

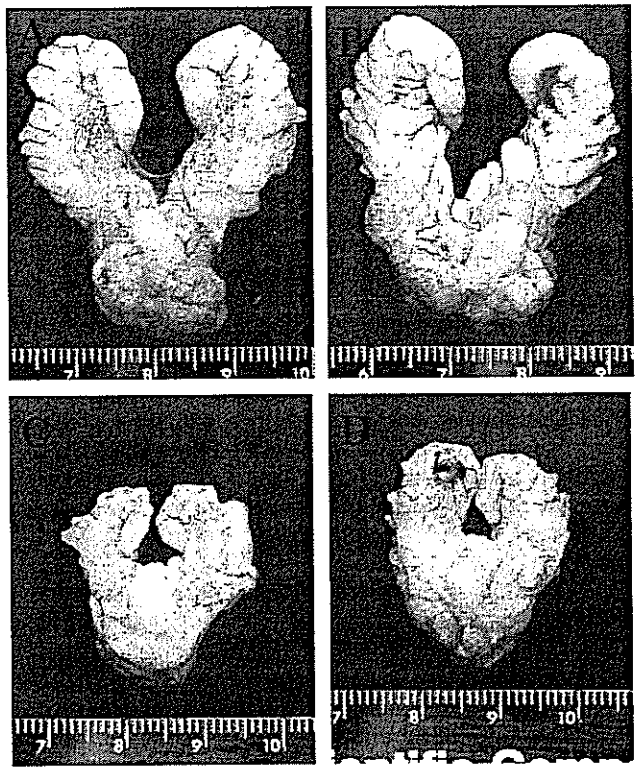

Fig. 1. Photomicrographs showing the macroscopic appearance of urogenital organs in the different groups after 15 weeks of treatment. (A) Controls; (B) vehicle-treated group; (C) low-dose leuprorelin group; (D) high-dose leuprorelin group. Macroscopically, prostates of the control and vehicle-treated rats showed irregular surfaces with no apparent nodule or mass formations. Treatment of rats with low and high doses of leuprorelin markedly reduced the gross weights of the prostate and seminal vesicle, with respect to control and vehicle-treated animals, without any significant difference between the two dose groups.

of prostatic adenocarcinomas in the ventral and lateral lobes (11.1 and 33.3%, and 11.1 and 22.2%, respectively) while causing non-significant change in the anterior lobe, with respect to controls. As for the dorsal prostate, complete inhibition of prostatic adenocarcinoma development was observed. However, no significant differences were found regarding the incidence of prostatic adenocarcinoma in the different prostatic lobes between the two dose groups.

Atrophic glands were also observed following treatment of transgenic rats with both doses of leuprorelin (Fig. 2), characterized by reduced epithelium and infiltration of inflammatory cells, most frequently observed in the high-dose group. Small cell carcinomas were also found in the lateral prostates of two rats (in the control and high-dose groups) and in the dorsal prostate of one rat (in the high-dose group).

Effects of leuprorelin treatment on androgen receptor and SV40 Tag protein expression

Expression of SV40 Tag and AR proteins was detected in almost all nuclei of the atypical epithelial cells of different prostatic lobes in the control and vehicle treated groups. Treatment of PB/SV40 Tag transgenic animals with low and high doses of leuprorelin acetate significantly reduced SV40 Tag expression in the ventral, dorsal and lateral lobes as well as AR expression in the dorsal prostate, compared to controls. Both SV40 Tag and AR expression was slightly decreased in the anterior prostate following leuprorelin treatment.

Effects of leuprorelin treatment on DNA synthesis in the ventral prostate of leuprorelin-treated rats

Subcutaneous administration of leuprorelin at low and high doses for 15 weeks to male PB/SV40 Tag transgenic rats caused significant parallel reduction in DNA synthesis in the epithelial cells of the ventral prostates compared to controls, as demonstrated by the decrease in the BrdU

Table 1. Statistical significance of the absolute and relative weight of urogenital organs (prostate, seminal vesicles and urinary bladder) as well as different prostatic lobes of PB/SV40 Tag transgenic rats treated with low and high doses of leuprorelin (15 weeks)

Group	No. of rats	Urogenital organs		Ventral prostate		Dorsolateral prostate		Anterior prostate and seminal vesicles	
		Absolute (g)	Relative (%)	Absolute (g)	Relative (%)	Absolute (g)	Relative (%)	Absolute (g)	Relative (%)
Control	9	5.33 ± 1.34	1.05 ± 0.24	0.58 ± 0.13	0.11 ± 0.02	1.48 ± 0.59	0.29 ± 0.11	3.15 ± 0.73	0.62 ± 0.13
Vehicle	9	5.03 ± 0.60	1.02 ± 0.16	0.48 ± 0.09	0.10 ± 0.02	1.22 ± 0.20	0.25 ± 0.05	3.01 ± 0.48	0.61 ± 0.12
Low-dose	9	1.71 ± 0.57*	0.35 ± 0.12*	0.14 ± 0.06*	0.03 ± 0.01*	0.53 ± 0.14*	0.11 ± 0.03*	0.94 ± 0.28*	0.19 ± 0.05*
High-dose	9	1.97 ± 0.81*	0.40 ± 0.15*	0.18 ± 0.07*	0.04 ± 0.01*	0.64 ± 0.23*	0.13 ± 0.05*	0.93 ± 0.50*	0.19 ± 0.09*

Values are mean ± SD. *Bonferroni's test was used for multiple comparisons, $P < 0.05$ is regarded as significant. Groups sharing the same characters are not significantly different.

Table 2. Incidence of prostatic adenocarcinomas in the different prostatic lobes of PB/SV40 Tag transgenic rats treated with low and high doses of leuprorelin (15 weeks)

Group	No of rats	Ventral			Lateral			Dorsal			Anterior	
		LG PIN	HG PIN	AC	LG PIN	HG PIN	AC	LG PIN	HG PIN	AC	PIN	AC
Control	9	0	0	9 (100%)	0	0	9 (100%)**	0	4 (44.4%)	5 (55.6%)	0	9 (100%)
Vehicle	9	0	0	9 (100%)	0	0	9 (100%)	0	3 (33.3%)	6 (66.7%)	0	9 (100%)
Low-dose	9	3 (33.3%)	5 (55.6%)	1 (11.1%)*	1 (11.1%)	7 (77.8%)	1 (11.1%)*	2 (22.2%)	7 (77.8%)	0*	3 (33.3%)	6 (66.7%)
High-dose	9	2 (22.2%)	4 (44.4%)	3 (33.3%)*	2 (22.2%)	5 (55.6%)	2 (22.2%)*,**	3 (33.3%)	6 (66.7%)	0*,**	2 (22.2%)	7 (77.8%)

*P value is significant at the 0.05 level by Scheffe's analysis. Groups sharing the same characters are not significantly different. **One case was diagnosed as small cell carcinoma. Percentage is shown in parentheses. AC, adenocarcinoma; HG PIN, high-grade prostatic intraepithelial; LG PIN, low-grade prostatic intraepithelial neoplasia.

doi: 10.1111/j.1349-7006.2006.00213.x

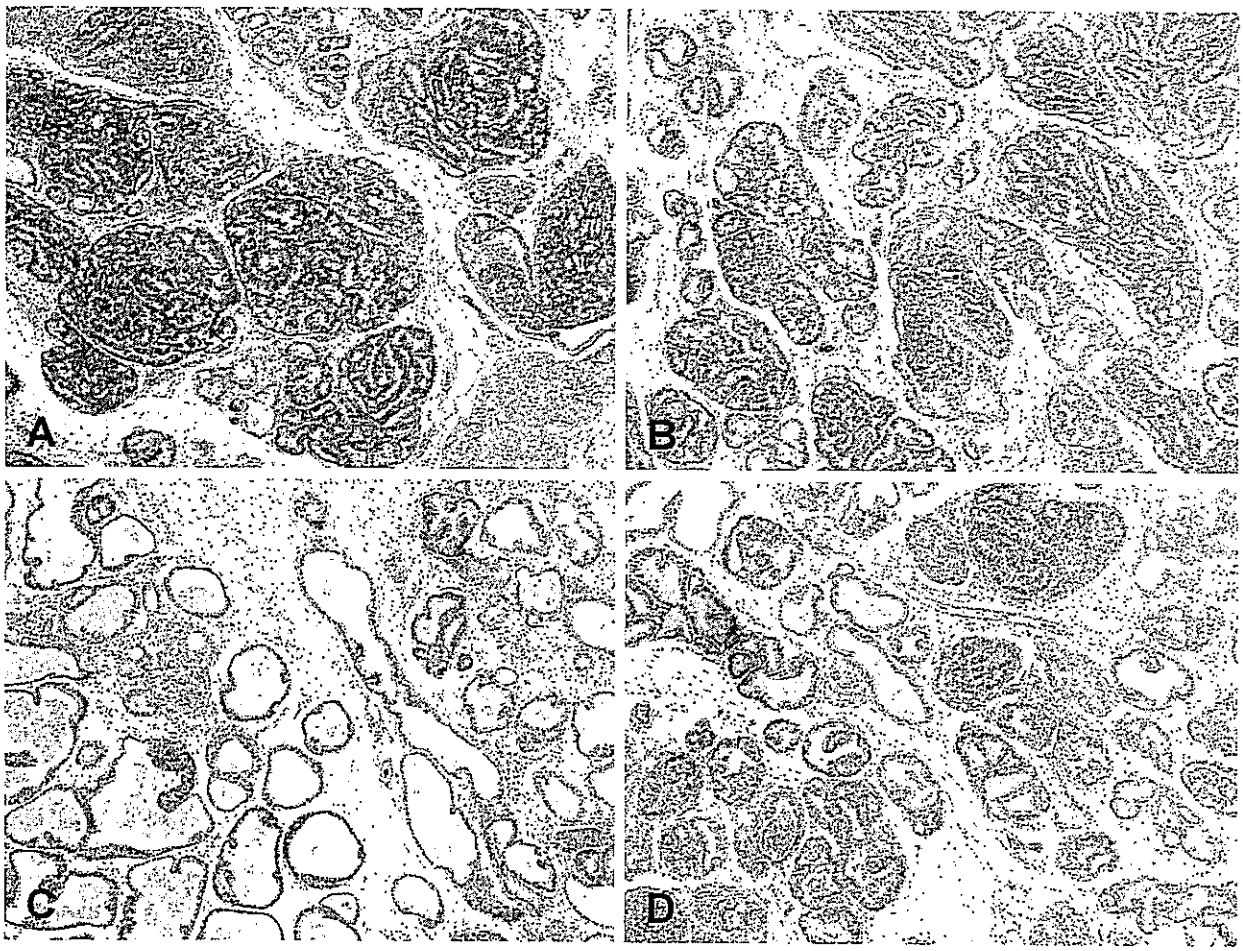

Fig. 2. Photomicrographs showing the histopathology of the ventral prostates of (A) control rats; (B) vehicle-treated group; (C) low-dose treated group; and (D) high-dose treated group. (A) and (B) show well-differentiated adenocarcinoma composed of atypical epithelial cells forming glandular and cribriform structures. (C) and (D) show that intraepithelial proliferation was markedly decreased and the relative volume of stroma was increased, prostatic intraepithelial neoplasia (PIN) is evident. Atrophic glands characterized by reduced epithelium with fibrosis and infiltration of inflammatory cells (including neutrophils, lymphocytes and macrophages) are also shown (hematoxylin and eosin, × 40).

labeling indices that reached 61.2% and 59.4%, respectively. However, no significant change in the BrdU labeling index was found between the two dose groups (Fig. 3).

Effects of leuprorelin treatment on quantitative expression of androgen receptor and SV40 Tag in the ventral prostate

RT-PCR results revealed that administration of low and high doses of leuprorelin for 15 weeks to PB/SV40 Tag transgenic rats produced a significant parallel reduction in the relative mRNA expression of SV40 Tag in the ventral prostates (87.3 and 80.0%, respectively) (Fig. 4), whereas AR expression was not significantly changed in comparison with controls (data not shown).

Effect of leuprorelin administration on the quantitative expression of LHRH-R in the pituitaries of PB/SV40 Tag transgenic rats

Expression of LHRH-R was reduced in the pituitaries of leuprorelin-treated animals, compared to untreated transgenic controls (Fig. 5). However, no significant differences were recorded in the aforementioned parameters with respect to untreated transgenic animals.

Effects of leuprorelin treatment on gene expression profiles in the ventral prostate of PB/SV40 Tag transgenic rats

Microarray analyses revealed 390 overexpressed and 655 downregulated genes (annotated and easily classified examples). Representative results are summarized in Tables 3 and 4.

Discussion

The present study demonstrated clear inhibitory effects of a LHRH agonist, leuprorelin acetate, on prostate oncogenesis in PB/SV40 Tag transgenic rats, in line with the conclusion that androgen ablation therapy continues to be the best approach for treatment of disseminated carcinomas of the prostate in the earliest androgen-responsive stages. Inhibition was achieved without any significant changes in total

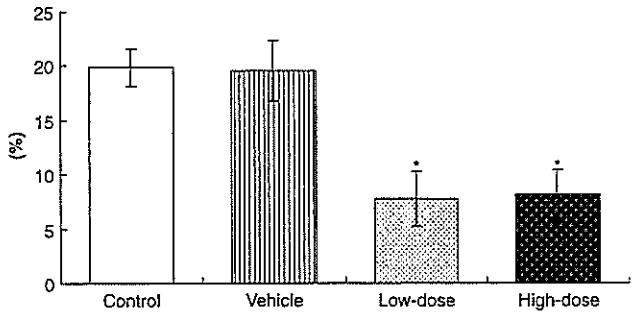

Fig. 3. Statistical significance of DNA synthesis (BrdU labeling indices) in epithelial cells of the ventral prostates of control, vehicle- and leuprorelin-treated PB/SV40 Tag transgenic rats. $*P < 0.05$ *versus* control and vehicle groups (Bonferroni's test). Values are mean ± SD.

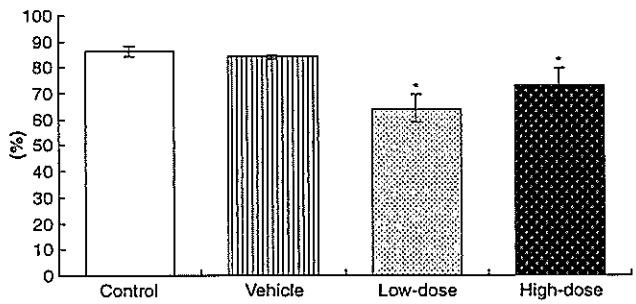

Fig. 4. Statistical significance of relative mRNA expression levels of SV40 Tag proteins compared with cyclophilin expression in the ventral prostates of control, vehicle- and leuprorelin-treated PB/SV40 Tag transgenic animals. $*P < 0.05$ *versus* control and vehicle groups (Bonferroni's test). Values are mean ± SE.

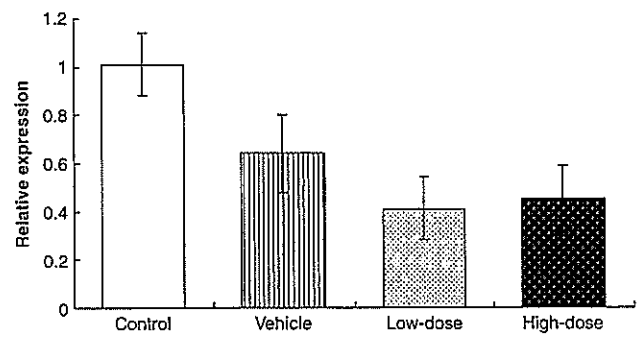

Fig. 5. Relative mRNA expression level of luteinizing hormone-releasing hormone receptor (LHRH-R) compared with cyclophilin expression in the pituitaries of untreated, vehicle- and leuprorelin-treated PB/SV40 Tag transgenic animals.Values are mean ± SE.

bodyweights and absolute or relative liver weights, so detrimental toxic effects were lacking. Histopathological examination revealed that treatment of 5-week old PB/SV40 Tag transgenic rats for 15 weeks with leuprorelin significantly reduced prostate adenocarcinoma progression in the ventral and lateral lobes, whereas complete inhibition was observed in the dorsal lobe in comparison with controls (Table 2). As shown, there are apparent lobe differences; however, the reasons are unknown. Our findings are in good agreement with previously reported studies demonstrating the inhibitory effect of leuprorelin treatment on the growth of the Dunning R 3327 androgen-sensitive rat prostatic tumor transplanted into adult male Copenhagen rats,[13] as well as the growth of male genital organs (testis, seminal vesicles and prostate) in intact Sprague Dawley male rats.[11] Multiple comparison analysis revealed that the action of leuprorelin was not enhanced at the higher dose, which is consistent with previously reported studies of leuprorelin dose dependence.[8,11]

Treatment of transgenic rats with low and high doses of leuprorelin produced a significant decrease in serum total testosterone level, but over 50% testosterone remained, while non-significant changes were recorded in serum LH and FSH levels, suggesting direct inhibitory effects on testicular steroidogenesis rather than indirect action through the pituitary-gonadal axis. These findings correlated well with the lack of any significant change in mRNA expression for LHRH receptors in the pituitaries of treated rats. Earlier animal studies revealed inhibition of testicular steroidogenesis in intact rats following leuprorelin treatment, with a subsequent decrease in the relative weight of rat reproductive organs.[6,14] Probable direct inhibitory effects of the drug on the prostate gland might exist in this transgenic strain, as evidenced by the detection of LHRH receptor mRNA expression in the ventral prostates of control and leuprorelin-treated animals by RT-PCR (data not shown). This possibility clearly warrants further investigation.

It is important to note that prostate cancer development and progression in the prostate adenoma in the TRAMP model as well as in our transgenic model is under the regulation of the androgen-dependent probasin promoter, which directs prostate-specific epithelial expression of the SV40 T antigen, an oncoprotein that interacts with retinoblastoma and p53 tumor-suppressor gene products.[9,15] Immunohistochemical and RT-PCR findings for SV40 Tag oncoprotein expression in the prostates of leuprorelin-treated animals showed a remarkable significant reduction in the ventral as well as dorsolateral lobes. DNA synthesis and proliferation of epithelial cells in neoplastic lesions in the ventral prostates were significantly reduced in leuprorelin-treated rats, as revealed by BrdU immunostaining and morphometric analysis of the percentage of relative epithelial areas. The lack of effects on AR protein expression as well as relative AR mRNA expression in the ventral prostates of leuprorelin-treated transgenic animals could be simply interpreted as reflecting reduction in serum androgen levels above the nadir level that would completely suppress production of ARs. We have already reported the effect of surgical castration on prostate tumor development in transgenic rats. Castration at an early stage induced an immature prostate gland structure and completely suppressed development of any neoplastic lesions, while castration at a late stage, that is, at the age of 20 weeks when adenocarcinomas had already developed, induced marked apoptosis of tumor cells leading to complete disappearance of carcinomas.[9] Compared to the previous data with surgical castration, the present data demonstrate suppression effects of leuprorelin to be rather mild and lobe specific. If suppression of testosterone was largely responsible, such lobe specificity would not be

doi: 10.1111/j.1349-7006.2006.00213.x

Table 3. Representative profile of some downregulated genes (<two-fold with respect to controls) in the ventral prostates of PB/SV40 Tag transgenic rats following treatment with a low leuprorelin dose

Function	GenBank no.	Gene name	Fold change
Apoptosis	NM_012922	Caspase 3 (Casp3)	0.48
	NM_053420	BCL2/adenovirus E1B 19 Kda-interacting protein 3 (Bnip3)	0.47
	NM_134334	Cathepsin D (Ctsd)	0.40
	NM_173114	Prostatic androgen-repressed message-1 (PARM-1)	0.39
	NM_012588	Insulin-like growth factor binding protein 3 (Igfbp3)	0.36
	NM_022277	Caspase 8 (Casp8)	0.33
	NM_031328	B-cell CLL/lymphoma 10 (Bcl10)	0.32
	NM_031735	Serine/threonine kinase 3 (Stk3)	0.31
	NM_017312	Bcl-2-realted ovarian killer protein (Bok)	0.26
	NM_021752	Apoptosis inhibitor (Api2)	0.25
	NM_031700	Claudin 3 (Cldn3)	0.22
	NM_031775	Caspase 6 (Casp6)	0.20
	NM_031098	Rho-associated kinase beta (Rock1)	0.05
Angiogenesis and invasion	NM_133523	Matrix metalloproteinase 3 (MMP3)	0.38
	U68726	Neogenin	0.34
	NM_031055	Matrix metalloproteinase 9 (MMP9)	0.31
	NM_012671	Transforming growth factor alpha (TGFA)	0.27
	NM_022221	Neutrophil collagenase (MMP8)	0.26
	NM_022603	Growth factor binding protein 1 (Fgfbp1)	0.23
	NM_022266	Connective tissue growth factor (Ctgf)	0.20
Cell cycle and growth	NM_171991	Cyclin B1 (Ccnb1)	0.49
	NM_012704	Prostaglandin E receptor 3 (Ptger3)	0.49
	NM_053464	Spermidine synthase (Srm)	0.42
	NM_053677	Protein kinase Chk2 (Rad53)	0.37
	NM_019219	Retinoblastoma-binding protein 9 (Rbbp9)	0.37
	NM_019296	Cell division cycle 2 homolog A (Cdc2a)	0.36
	NM_013015	Prostaglandin D2-synthase (Ptgds)	0.35
	NM_080400	Checkpoint kinase 1 homolog (Chek 1)	0.32
	NM_021740	Prothymosin alpha (Ptma)	0.28
	NM_031094	Retinoblastoma-like 2 (Rbl2)	0.25
	NM_199501	Cyclin dependent kinase 2 (Cdk2)	0.25
	NM_021583	Prostaglandin E synthase (Ptges)	0.25
	NM_052981	Cyclin H (Ccnh)	0.24
	NM_022381	Proliferating cell nuclear antigen (Pcna)	0.17
Cell signaling	NM_177933	Sel1 (Suppressor of lin-12) 1 homolog (Sel1h)	0.49
	NM_017020	Interleukin 6 receptor (Il6r)	0.48
	NM_017071	Insulin receptor (Insr)	0.47
	NM_012747	Signal transducer and activator of transcription 3 (Stat3)	0.46
	NM_130405	Src associated in mitosis (Sam68)	0.46
	NM_022532	v-raf murine sarcoma 3611 viral oncogene homolog 1 (Araf1)	0.45
	L26267	Nuclear factor Kappa B p105 subunit mRNA (NFkB)	0.44
	NM_012514	Breast cancer 1 (Brca1)	0.43
	NM_057211	Kruppel-like factor 9 (Klf9)	0.43
	NM_017218	Avian erythroblastosis oncogene B3 (Erbb3)	0.41
	NM_031514	Janus kinase 2 (Jak2)	0.38
	NM_013145	Guanine nucleotide binding protein, alpha inhibiting 1 (Gnai1)	0.37
	AF231407	Calmodulin III (Calm3)	0.34
	NM_031338	Ca^{++}/calmodulin-dependent protein kinase kinase beta (Cam2KK)	0.32
	NM_017198	p21-activated kinase 1 (Pak1)	0.28
	NM_012499	Adenomatosis polyposis coli (Apc)	0.28
	NM_053777	Mitogen activated protein kinase 8 interacting protein (Mapk8ip)	0.27
	NM_033230	v-akt murine thymoma viral oncogene homolog 1 (Akt1)	0.26
	NM_031143	Diacylglycerol kinase zeta (Dgkz)	0.23
	NM_013022	Rho-associated coiled-coil forming kinase 2 (Rock2)	0.18
	NM_053357	Beta-catenin (Catnb)	0.10
Replication, DNA repair, transcription and translation	NM_053857	Eukaryotic translation initiation factor 4E binding protein 1 (Eif4ebp1)	0.49
	NM_031772	RNA polymerase I (Rpo1–4)	0.45
	NM_171995	Damage-specific DNA binding protein 1 (Ddb1)	0.45
	XM_234239	DNA repair endonuclease	0.44
	NM_012866	Nuclear transcription factor-Y gamma (Nfyc)	0.44
	NM_021662	DNA polymerase delta, catalytic subunit (Pold1)	0.43

Table 3. *continued*

Function	GenBank no.	Gene name	Fold change
	NM_053480	DNA polymerase alpha subunit II (Pola2)	0.42
	NM_031340	Timeless homolog (Timeless)	0.41
	NM_133609	Eukaryotic translation initiation factor2B, subunit 3 (Eif2b3)	0.41
	NM_022397	Ribonucleoprotein F (Hnrpf)	0.39
	NM_138873	Nibrin (Nbn, p95)	0.39
	NM_031058	Mismatch repair protein (Msh2)	0.32
	NM_031107	S6 protein kinase (Rsk-1)	0.30
	NM_031599	Eukaryotic translation initiation factor 2 alpha kinase 3 (Eif2ak3)	0.29
	NM_053528	DNA polymerase gamma (Polg)	0.23
	NM_017141	DNA polymerase beta (Polb)	0.21
	NM_138866	Initiation factor (eIF-2be)	0.17
	AJ011608	DNA polymerase alpha subunit IV primase	0.05
Secretory activity	NM_012836	Carboxypeptidase D (cpd)	0.49
	NM_017284	Proteasome subunit, beta type 2 (Psmb2)	0.48
	NM_022219	Alpha 1,3-fucosyltransferase (Fuc-T)	0.46
	NM_024151	ADP-ribosylation factor 4 (Arf4)	0.41
	NM_053406	Protein O-mannosyltransferase 1 (Pomt1)	0.33
	AF102262	N-acetylglucosamine galactosyltransferase (beta1-4GT)	0.29
	NM_021869	Syntaxin 7 (Stx7)	0.27
	NM_031722	Coated vesicle membrane protein	0.24
	NM_019364	Vesicle transport-related	0.22
Metabolism	NM_012941	Cytochrome P450, subfamily 51 (Cyp51)	0.49
	NM_013134	3-hydroxy-3-methylglutaryl-coenzyme A reductase (Hmgcr)	0.47
	NM_080886	Sterol-C4-methyloxidase-like (Sc4mol)	0.43
	NM_012621	6-phosphofructo-2-kinase/fructose-2,6-biphosphatase 1 (Pfkfb1)	0.36
	NM_053291	Phosphoglycerate kinase 1 (Pgk1)	0.36
	NM_024381	Glycerol kinase (Gyk)	0.33
	NM_031118	Acyl-coenzyme A: cholesterolacyltransferase (Soat1)	0.31
	NM_023104	Acetoacetyl-CoA synthetase	0.31
	NM_017136	Squalene epoxidase (Sqle)	0.30
	NM_030992	Phospholipase D1 (Pld1)	0.28
	NM_012851	Hydroxysteroid 17β-dehydrogenase 1 (Hsd17b1)	0.26
	NM_198738	Phosphoserine aminotransferase 1 (Psat1)	0.21
	NM_172062	Prolyl 4-hydroxylase α subunit (P4ha1)	0.18
	NM_031043	Glycogenin (Gyg)	0.14
	NM_021751	Prominin (Prom)	0.14
Miscellaneous	NM_053946	Implantation-associated protein (IAG2)	0.49
	NM_012548	Endothelin 1 (Edn1)	0.47
	NM_199266	Cystatin related protein 2	0.44
	NM_022391	Pituitary tumor-transforming 1 (Pttg1)	0.43
	NM_022298	Alpha-tubulin (Tuba1)	0.40
	NM_031821	Serum-inducible kinase (Snk)	0.38
	NM_173102	Tubulin, beta (Tubb5)	0.38
	NM_199370	Keratin 8 (Krt8)	0.30
	NM_012715	Adrenomedullin (Adm)	0.17
	NM_175759	Kallikrein, submaxillary gland S3 (rK9, K1k9)	0.15
	NM_012718	Androgen regulated 20 KDa protein (Andpro)	0.08

expected as with surgical castration. Those findings support our speculation that suppression of tumor development in the present work was partly due to specific effects of the LH-RH agonist.

Our results thus suggest that inhibition of prostatic adenocarcinoma development in the ventral, dorsal and lateral prostates of PB/SV40 Tag transgenic rats by leuprorelin treatment was mainly due to downregulation of SV40 Tag oncoprotein expression and partly due to reduction of the serum androgen level. In addition, some androgen-independent mechanisms resulting in reduction of cell proliferation and regression of prostate cancers might be involved. The present microarray analysis indicated that many kinds of genes, including examples involved in apoptosis, angiogenesis, the cell cycle and growth, were influenced by leuprorelin.

In conclusion, the LHRH agonist leuprorelin acts to inhibit prostate carcinogenesis in PB/SV40 Tag transgenic rats by multiple mechanisms including reduction of testosterone biosynthesis, suppression of SV40 Tag oncoprotein expression and alteration in the expression of many genes that are critically involved in the control of cell proliferation and cell cycle progression, transcription and translation, signaling, angiogenesis and invasion, metabolism and cytoskeleton formation. This study also confirmed the suitability of the rat

doi: 10.1111/j.1349-7006.2006.00213.x

Table 4. Representative profile of some overexpressed genes (>two-fold with respect to controls) in the ventral prostates of PB/SV40 Tag transgenic rats following treatment with a low leuprorelin dose

Miscellaneous	NM_053968	Metallothionein 3 (Mt3)	7.66
	NM_012657	Serine protease inhibitor (Spin2b)	6.79
	NM_145774	Rab38, member of RAS oncogene family	3.93
	NM_012774	Glypican 3 (Gpc3)	3.57
	NM_012580	Inhibin alpha (Inha)	3.50
	NM_144737	Flavin-containing monooxygenase 2 (Fmo2)	3.03
	NM_012662	Seminal vesicle protein 4 (Svp4)	2.82
	NM_012789	Dipeptidyl peptidase 4 (Dpp4)	2.74
	NM_024136	Epididymal retinoic acid-binding protein (Erabp)	2.39
	NM_080479	Melanoma antigen, family D, 2 (Maged2)	2.35
	NM_053348	Fetuin beta (Fetub)	2.30
	NM_139104	Estrogen-regulated protein CBL20, 204 KD	2.23
	NM_199119	DEAD (Asp-Glu-Ala-Asp) box polypeptide 24 (Ddx24)	2.09
	NM_012880	Superoxide dismutase 3 (Sod3)	2.04

SV40 Tag model for prostate cancer chemoprevention and chemotherapeutic studies.

Acknowledgments

This work was performed through collaboration between the Japanese Government represented by Professor Tomoyuki Shirai (Department of Experimental Pathology and Tumor Biology, Nagoya City University Graduate School of Medical Sciences, Nagoya, Japan) and the Egyptian Government represented by Professor Fawzia M. Refaie (Department of Biochemistry, Faculty of Science, Ain Shams University, Cairo, Egypt). The authors would like to thank Takeda Chemical Industries (Osaka, Japan) for providing the leuprorelin acetate microcapsule sustained-release preparation.

References

1 Stewart SL, King JB, Thompson TD, Friedman C, Wingo PA. Cancer mortality surveillance – United States, 1990–2000. *MMWR Surveill Summ* 2004; 53: 1–108.
2 Lau HL, Zhu XM, Leung PC *et al.* Detection of mRNA expression of gonadotropin-releasing hormone and its receptor in normal and neoplastic rat prostates. *Int J Oncol* 2001; 19: 1193–201.
3 Tieva A, Bergh A, Damber JE. The clinical implications of the difference between castration, gonadotrophin releasing-hormone (GnRH) antagonists and agonist treatment on the morphology and expression of GnRH receptors in the rat ventral prostate. *BJU Int* 2003; 91: 227–33.
4 Limonta P, Moretti RM, Marelli MM, Dondi D, Parenti M, Motta M. The luteinizing hormone-releasing hormone receptor in human prostate cancer cells: messenger ribonucleic acid expression, molecular size, and signal transduction pathway. *Endocrinology* 1999; 140: 5250–6.
5 Halmos G, Arencibia JM, Schally AV, Davis R, Bostwick DG. High incidence of receptors for luteinizing hormone-releasing hormone (LHRH) and LHRH receptor gene expression in human prostate cancers. *J Urol* 2000; 163: 623–9.
6 Okada H, Doken Y, Ogawa Y, Toguchi H. Sustained suppression of the pituitary-gonadal axis by leuprorelin three-month depot microspheres in rats and dogs. *Pharm Res* 1994; 11: 1199–203.
7 Periti P, Mazzei T, Mini E. Clinical pharmacokinetics of depot leuprorelin. *Clin Pharmacokinet* 2002; 41: 485–504.
8 Chrisp P, Sorkin EM, Leuprorelin. A review of its pharmacology and therapeutic use in prostatic disorders. *Drugs Aging* 1991; 1: 487–509.
9 Asamoto M, Hokaiwado N, Cho YM *et al.* Prostate carcinomas developing in transgenic rats with SV40 T antigen expression under probasin promoter control are strictly androgen dependent. *Cancer Res* 2001; 61: 4693–700.
10 Nakatani T, Roy G, Fujimoto N, Asahara T, Ito A. Sex hormone dependency of diethylnitrosamine-induced liver tumors in mice and chemoprevention by leuprorelin. *Jpn J Cancer Res* 2001; 92: 249–56.
11 Gotanda K, Shinbo A, Okada M *et al.* Effects of combination therapy with a luteinizing hormone-releasing hormone agonist and chlormadinone acetate on rat prostate weight and plasma testosterone levels. *Prostate Cancer Prostatic Dis* 2003; 6: 66–72.
12 Kawabe M, Shibata MA, Sano M *et al.* Decrease of prostaglandin E2 and 5-bromo-2′-deoxyuridine labeling but not prostate tumor development by indomethacin treatment of rats given 3,2′-dimethyl-4-aminobiphenyl and testosterone propionate. *Jpn J Cancer Res* 1997; 88: 350–5.
13 Ichikawa T, Akimoto S, Shimazaki J. Effect of leuprolide on growth of rat prostatic tumor (R 3327) and weight of male accessory sex organs. *Endocrinol Jpn* 1988; 35: 181–7.
14 Ogawa Y, Okada H, Heya T, Shimamoto T. Controlled release of LHRH agonist, leuprolide acetate, from microcapsules: serum drug level profiles and pharmacological effects in animals. *J Pharm Pharmacol* 1989; 41: 439–44.
15 Asamoto M, Hokaiwado N, Cho YM, Shirai T. Effects of genetic background on prostate and taste bud carcinogenesis due to SV40 T antigen expression under probasin gene promoter control. *Carcinogenesis* 2002; 23: 463–7.

Available online at www.sciencedirect.com
SCIENCE DIRECT®
Cancer Letters 210 (2004) 159–169
CANCER Letters
www.elsevier.com/locate/canlet

Preventive effects of extract of leaves of ginkgo (*Ginkgo biloba*) and its component bilobalide on azoxymethane-induced colonic aberrant crypt foci in rats

Rikako Suzuki[a,b,*], Hiroyuki Kohno[a], Shigeyuki Sugie[a], Keiko Sasaki[c], Teruki Yoshimura[c], Keiji Wada[c], Takuji Tanaka[a]

[a]*The First Department of Pathology, Kanazawa Medical University, 1-1 Daigaku, Uchinada, Ishikawa 920-0293, Japan*
[b]*Research Fellow of the Japan Society for the Promotion of Science, 6 Ichibancho, Chiyoda-ku, Tokyo 102-8471, Japan*
[c]*Department of Hygienic Chemistry, Faculty of Pharmaceutical Sciences, Health Sciences University of Hokkaido, Kanazawa 1757, Ishikari-Tobetsu, Hokkaido 061-0293, Japan*

Received 17 November 2003; received in revised form 21 January 2004; accepted 28 January 2004

Abstract

The modifying effects of dietary feeding of extract of leaves of ginkgo (*Ginkgo biloba*) (EGb) and bilobalide isolated from EGb on the development of azoxymethane (AOM)-induced colonic aberrant crypt foci (ACF) were investigated in male F344 rats. We also assessed the effects of EGb and bilobalide on proliferating cell nuclear antigen (PCNA) index in 'normal-appearing' crypts and activities of detoxifying enzymes of cytochrome P450 (CYP), glutathione *S*-transferase (GST) and quinine reductase (QR) activity in the liver. To induce ACF, rats were given two weekly subcutaneous injections of AOM (20 mg/kg body wt). They also received the experimental diets containing EGb (50 or 500 ppm) and bilobalide (15 or 150 ppm) for 4 weeks, starting 1 week before the first dosing of AOM. AOM exposure produced a substantial number of ACF (106 ± 10) at the end of the study (week 4). Dietary administration of EGb and bilobalide caused significant reduction in the frequency of ACF: 50 ppm EGb, 73 ± 17 (31% reduction, $P < 0.001$); 500 ppm EGb, 56 ± 13 (47% reduction, $P < 0.001$); 15 ppm bilobalide, 79 ± 17 (25% reduction, $P < 0.01$); and 150 ppm bilobalide, 71 ± 30 (33% reduction, $P < 0.01$). Immunohistochemically, EGb or bilobalide administration significantly lowered PCNA index in normal-appearing crypts. Feeding with EGb or bilobalide increased activities of CYP as well as GST and QR in the liver. These findings might suggest possible chemopreventive ability of EGb or bilobalide, through alterations in cryptal cell proliferation activity and drug metabolizing enzymes' activities, in colon tumorigenesis.

Keywords: *Ginkgo biloba* L; Bilobalide; Aberrant crypt foci: inhibition; Rat colon

Abbreviations: EGb, Extract of *Ginkgo biloba* leaves; AOM, Azoxymethane; ACF, Aberrant crypt foci; PCNA, Proliferating cell nuclear antigen; CYP, Cytochrome P450; GST, Glutathione *S*-transferase; QR, Quinone reductase; ACs, Aberrant crypts; COX-2, Cyclooxygenase-2; SOD, Superoxide dismutase; iNOS, Inducible nitric oxide synthase.

* Corresponding author. Address: The First Department of Pathology, Kanazawa Medical University, 1-1 Daigaku, Uchinada, Ishikawa 920-0293, Japan. Tel.: +81-76-286-2211; fax: +81-76-286-6926.
E-mail address: rikako@kanazawa-med.ac.jp (R. Suzuki).

0304-3835/$ - see front matter © 2004 Elsevier Ireland Ltd. All rights reserved.
doi:10.1016/j.canlet.2004.01.034

1. Introduction

Herbal medicines (defined as preparations derived from plants or fungi, for example by alcoholic extraction or decoction, used to prevent and treat diseases) are an essential part of traditional medicine in almost any culture [1]. Recently, the attention to herbal medicines as alternative medical treatment is increasing, and in industrialized countries herbal drugs and supplements are an important market. Ginkgo (*Ginkgo. biloba*) is one of the popular herbal medicines, and extracts from its leaves have been used for food supplement or health food without any restriction in Japan as well as the United State. Additionally, in many European countries this extracts have been clinically used [2–5].

Extract from leaves of ginkgo (*Ginkgo biloba*) (EGb) includes flavonoid glycosides, diterpenes (ginkgolides A, B, C and M) and a sesquiterpene (bilobalide, Fig. 1) as active ingredients [6], and isolated constituents have been found to be active in a variety of assays. For example, ginkgolide B has a potent platelet activating factor antagonist [7,8], bilobalide protects cultured rat hippocampal neurons against damage caused by glutamate [9], and the flavonoid fraction contains free radical scavengers [10]. Other biological effects of EGb have also been reported: it attenuates ischemia/reperfusion damage of brain tissue [11,12] and enhances brain functions including learning and memory [13]. Also, it may help people with Alzheimer or dementia to become more alert, sociable, feel better, and think more clearly [3,14]. However, chemopreventive efficacy of EGb in carcinogenesis or antiproliferative ability of EGb in cancer cells has been evaluated in a few studies [15,16].

Cytochrome P450 (CYP) isoenzymes are one major kind of phase I enzymes and play an important role in the oxidation of procarcinogens, often resulting in the formation of highly reactive compounds that are the ultimate carcinogens [17]. GST and QR are phase II enzymes and responsible for catalyzing the biotransformation of a variety of electrophiles. They have a central role in the detoxification of activated metabolites of procarcinogens produced by phase I with some exception.

In the present study, we investigated the possible inhibitory effect of EGb and bilobalide, one of the effective constituents of EGb, on the development of azoxymethane (AOM)-induced aberrant crypt foci (ACF), which are putative preneoplastic lesions for colonic adenocarcinoma [18–20], with a short-term rat ACF bioassay to predict their cancer chemopreventive ability in large bowel. In addition, we evaluated the proliferating cell nuclear antigen (PCNA) index to assess whether EGb or bilobalide affects cell proliferation activity in colonic mucosa, since certain chemopreventive agents exerts their inhibitory action through reduction of the cell proliferating activity in the target tissues [21]. Also, we measured the activities of cytochrome P450 (CYP), glutathione *S*-transferase (GST) and quinone reductase (QR) activity in the liver.

2. Material and methods

2.1. Animals, chemicals and diets

Male F344 rats (Charles River Japan, Inc , Kanazawa, Japan) aged 5 weeks were used for an ACF assay. The animals were maintained in Kanazawa Medical University Animal Facility according to the Instrumentional Animal Care Guidelines. All animals were housed in plastic cages (4 rats/gage) with free access to tap water and basal MF diet (Oriental Yeast, Co., Ltd., Nagoya, Japan), under controlled conditions of humidity (50 ± 10%), lightning (12-h light/dark cycle) and temperature (23 ± 2 °C). They were quarantined for 7 days and randomized by body weight into experimental and control groups. AOM for ACF induction was purchased from Sigma Chemical Co. (St Louis, MO, USA). EGb was provided by Schwabe Greenwave (Tokyo, Japan) and bilobalide was isolated from EGb as described previously with some modifications [22]. Bilobalide was identified by its spectral data, which was identical to described in the literature [23].

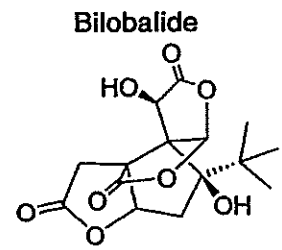

Fig. 1. Chemical structure of bilobalide.

Powdered MF diet was used as basal diet throughout the study. Experimental diet was made by mixing EGb (50 or 500 ppm) or bilobalide (15 or 150 ppm) in the powdered basal diet using a rocking mixer (RM-10-2, Aichi Electric Co., Ltd., Kasugai City, Japan).

2.2. Experimental procedure for ACF assay

A total of 56 male F344 rats were divided into seven experimental and control groups (Fig. 2). Animals in groups 1 through 5 was initiated with AOM by two weekly subcutaneous injections (20 mg/kg body weight). Rats in groups 2 and 3 were fed the diets containing 50 and 500 ppm EGb for 4 weeks, respectively, starting one week before the first dosing with AOM. Similarly, animals in groups 4 and 5 were fed the diets mixed with 15 and 150 ppm bilobalide for 4 weeks, respectively. Groups 6 and 7 did not receive AOM and were given the diets containing 500 ppm EGb and 150 ppm bilobalide, respectively. Group 8 served as untreated control. Rats sacrificed under ether anesthesia at week 4 to assess the occurrence of colonic ACF. They underwent careful necropsy, with emphasis on the colon, liver, kidney, lung, and heart. All grossly abnormal lesions in any tissue, and the organs such as liver (caudate lobe), kidney, lung, and heart were fixed in 10% buffered formalin solution.

2.3. Determination of ACF

The frequency of ACF was determined according to the method described in our previous report [24] At necropsy, the colons were flushed with saline, excised, cut open longitudinally along the main axis, and then washed with saline. They were cut and fixed in 10% buffered formalin for at least 24 h. Fixed colons were dipped in a 0.5% solution of methylene blue in distilled water for 30 s, briefly washed with the distilled water, and placed on a microscope slide for counting ACF.

2.4. PCNA Immunohistochemistry

Immunohistochemical staining for PCNA was performed by the avidin-biotin complex method (Vecstain Elite ABC Kit, Vector, Burlingame, CA). Tissue sections were deparaffinized with xylene, hydrated through a graded ethanol series, immersed in 0.3% hydrogen peroxide in absolute methanol for

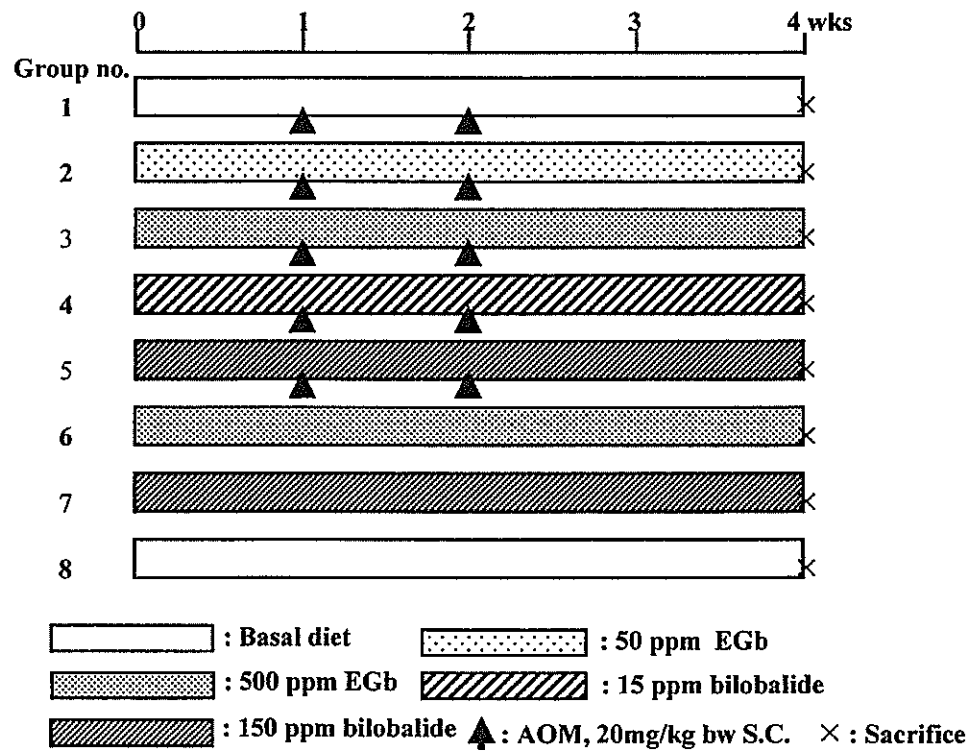

Fig. 2. Experimental protocol.

30 min at room temperature to block endogenous peroxidase activity, and then washed in phosphate-buffered saline (pH 7.2). Following incubation with normal rabbit serum at room temperature for 10 min to block background staining, the sections were incubated with an anti-PCNA antibody (mouse monoclonal PC10, Dako Co., Kyoto; 1:100 dilution) for 12 h in a humidified chamber at room temperature. They were then reacted with 3,3′-diaminobenzidine and lightly counterstained with Harris' hematoxylin. For determination of PCNA-positive index, 10 full-length crypts of each colon were examined. The number and the position of PCNA positively stained nuclei in each crypt column were recorded and expressed as PCNA-positive index (number of positive stained nuclei × 100/total number of nuclei counted). The observer was unaware of the group to which the specimens belonged.

2.5. Measurement of drug metabolizing enzymes in rat liver

The liver without caudate lobe was rinsed in cold 0.9% NaCl, homogenized in ice–cold 50 mM Tris buffer (pH 7.4) containing 0.15 M KCl to yield a 10% (wt/vol) homogenate, and then centrifuged at 10,000 × g for 60 min at 4 °C. The supernatant (cytosol fraction), after discarding any floating lipid layer and appropriate dilution, was used for enzyme assays.

The concentration of total amount of CYP and cytochrome b_5 were quantified by the method of Omura and Sato [25]. NADPH- cytochrome P450 reductase activity was measured by the method of Phillips et al. [26]. For measurement of activities of CYP1A1 and CYP1A2 levels using ethoxyresorufin *O*-deethylase and methoxyresorufin *O*-demethylase as substrate, respectively [27,28]. *p*-Nitrophenol hydroxylase and testosterone 6β-transferase activities were used to determine CYP 2E1 [29] and CYP3A [30], respectively.

The cytosolic GST activity was determined spectrophotometrically at 340 nm with 1-chloro-2,4-dinitrobenzene as a substrate according to the procedure of Habig et al. [31]. QR was determined spectrophotometrically by measuring the decrease in cytochrome c at 550 nm by the method of Ernster [32].

2.6. Statistical evaluation

Where applicable, data were analyzed using Student' *t*-test or Welch's *t*-test with $P < 0.05$ as the criterion of significance.

3. Results

3.1. General observation

All animals remained healthy throughout the experimental period. Food consumption (g/day/rat) did not differ significantly among the group (data not shown). Body, liver, and relative liver weights (g/100 g body weight) in all groups are shown in Table 1. At the end of the study, the mean body weight

Table 1
Body, liver, and relative liver weights

Group no.	Treatment (no. of rats examined)	Body wt (g)	Liver wt (g)	Relative liver wt (g/100 g body wt)
1	AOM alone (8)	207 ± 6[a]	9.7 ± 0.6	4.69 ± 0.14
2	AOM + 50 ppm EGb (8)	210 ± 7	10.9 ± 0.4[b]	5.20 ± 0.20[b]
3	AOM + 500 ppm EGb (8)	209 ± 9	11.9 ± 0.6[b]	5.68 ± 0.18[b]
4	AOM + 15 ppm bilobalide (8)	212 ± 9	12.0 ± 0.5[b]	5.66 ± 0.18[b]
5	AOM + 150 ppm bilobalide (8)	214 ± 9	13.4 ± 0.7[b]	6.27 ± 0.25[b]
6	500 ppm EGb (4)	223 ± 10	12.1 ± 0.4[c]	5.46 ± 0.27[d]
7	150 ppm bilobalide (4)	226 ± 7[d]	13.5 ± 0.9[c]	5.94 ± 0.29[c]
8	No treatment (4)	214 ± 7	10.7 ± 0.6	4.97 ± 0.20

[a] Mean ± SD.
[b] Significantly different from group 1 by Welch's *t*-test or Student's *t*-test ([b]$P < 0.001$).
[c] Significantly different from group 8 by Welch's *t*-test or Student's *t*-test $P < 0.001$).
[d] Significantly different from group 8 by Welch's *t*-test or Student's *t*-test ([c]$P < 0.01$).

Table 2
Effect of EGb and bilobalide on AOM-induced ACF formation in male F344 rats

Group no.	Treatment (no. of rats examined) (%)	Incidence (%)	Total no. of ACF/colon (%)	Total no. of ACs/colon (%)	No. of aberrant crypts/focus (%)	% of ACF containing 4 or more ACs
1	AOM alone (8)	8/8 (100)	106 ± 10[a] (100)	220 ± 23 (100)	2.07 ± 0.07 (100)	9.2 ± 1.3 (100)
2	AOM + 50 ppm EGb (8)	8/8 (100)	73 ± 17[b] (69)	126 ± 30[b] (57)	1.73 ± 0.17[b] (84)	2.2 ± 3.1[c] (24)
3	AOM + 500 ppm EGb (8)	8/8 (100)	56 ± 13[b] (53)	94 ± 26[b] (43)	1.67 ± 0.09[b] (81)	1.5 ± 1.6[b] (16)
4	AOM + 15 ppm bilobalide (8)	8/8 (100)	79 ± 17[d] (75)	136 ± 33[b] (62)	1.70 ± 0.07[b] (82)	1.9 ± 2.1[b] (21)
5	AOM + 150 ppm bilobalide (8)	8/8 (100)	71 ± 30[d] (67)	119 ± 53[b] (54)	1.68 ± 0.12[b] (81)	2.0 ± 1.3[b] (22)
6	500 ppm EGb (4)	0/4 (0)	0	0	0	0
7	150 ppm bilobalide (4)	0/4 (0)	0	0	0	0
8	No treatment (4)	0/4 (0)	0	0	0	0

[a] Mean ± SD.
[b] Significantly different from group 1 by Welch's *t*-test or Student's *t*-test ($P < 0.001$).
[c] Significantly different from group 1 by Welch's *t*-test or Student's *t*-test ($P < 0.005$).
[d] Significantly different from group 1 by Welch's *t*-test or Student's *t*-test ($P < 0.01$).

of group 7 (150 ppm bilobalide alone) was significantly greater than those of group 8 (untreated) ($P < 0.01$). The mean liver and relative liver weights of groups 2 (AOM + 50 ppm EGb), 3 (AOM + 500 ppm EGb), 4 (AOM + 15 ppm bilobalide), and 5 (AOM + 150 ppm bilobalide) were greater than those of group 1 (AOM alone) ($P < 0.001$). The mean liver weights of groups 6 (500 ppm EGb alone) and 7 (150 ppm bilobalide alone) were greater than group 8 (untreated) ($P < 0.001$). Similarly the relative liver weights of groups 6 and 7 were greater than group 8 ($P < 0.01$ and $P < 0.001$, respectively). However, no significant pathological alternations were found in any organs, including the liver.

3.2. Frequency of ACF

Table 2 summarizes the data on colonic ACF formation (Fig. 3). All rats belonging to groups 1 through 5, which were treated with AOM, developed

Fig. 3. Morphology of ACF. (a) ACF (arrows) on methylene-blue-stained colonic mucosa of a rat in group 1 and (b) ACF on hematoxylin and eosin-stained section from a rat in group 1.

ACF. The mean number of ACF/ colon in group 1 was 106 ± 10. The dietary administration with EGb (groups 2 and 3) or bilobalide (groups 4 and 5) significantly reduced the ACF incidence compared to group 1: 73 ± 17 (31% reduction, $P < 0.001$) at a dose level of 50 ppm EGb (group 2), 56 ± 13 (47% reduction, $P < 0.001$) at a dose level of 500 ppm EGb (group 3), 79 ± 17 (25% reduction, $P < 0.01$) at a dose level of 15 ppm bilobalide (group 4), 71 ± 30 (33% reduction, $P < 0.01$) at a dose level of 150 ppm bilobalide (group 5). Additionally, there were significant decreases in the total number of aberrant crypts (ACs) per colon ($P < 0.001$) and the number of ACs per focus ($P < 0.001$) in these groups. Also, the percentage of ACF consisting of more than 4 crypts in these groups were significantly smaller than that of group 1 (group 2 vs. group 1, $P < 0.005$; groups 3, 4 or 5 vs. group 1, $P < 0.001$). In groups 6, 7 and 8, there was no microscopically observable change, including ACF, in colonic morphology.

3.3. PCNA-labeling index in 'normal-appearing' and normal colonic crypts

The PCNA-labeling indices in colonic mucosa are presented in Table 3. Dietary feeding with EGb or bilobalide significantly reduced the mean PCNA-labeling indices in 'normal-appearing' crypts when compared with group 1 (group 2 or 5 vs. group 1, $P < 0.01$; group 3 vs. group 1, $P < 0.001$; group 4 vs. group 1, $P < 0.005$). Feeding with 500 ppm EGb alone (group 6) or 150 ppm bilobalide alone (group 7) did not affect the PCNA-labeling index in 'normal-appearing' crypts of rats, when compared with that of untreated rats (group 8).

3.4. Effects of EGb and bilobalide on content and activity of CYP

Rats given the diets containing either EGb or bilobalide increased the content of CYP or cytochrome b_5 and the activity of NADPH- cytochrome P450 reductase in the liver (Table 4). A significant increase in CYP was detected in the groups given the diets containing bilobalide at the concentrations of 15 ppm (group 4, 0.61 ± 0.09, $P < 0.005$) and 150 ppm (group 5, 0.91 ± 0.20, $P < 0.05$) along with AOM injection when compared to group 1 (AOM alone, 0.39 ± 0.04). Also, the value in the group given the diet containing 500 ppm EGb (group 6, 0.66 ± 0.05, $P < 0.001$) or 150 ppm bilobalide (group 7, 1.15 ± 0.13, $P < 0.001$) alone was significantly greater than group 8 (no treatment, 0.35 ± 0.08). As for cytochrome b_5, significantly increase was identified in the groups given AOM + 500 ppm EGb (0.48 ± 0.03, $P < 0.001$), AOM + 15 ppm bilobalide (0.46 ± 0.02, $P < 0.001$) and AOM + 150 ppm bilobalide (0.57 ± 0.09, $P < 0.005$) when compared to group 1 (0.33 ± 0.03). In addition, treatment with 500 ppm EGb (0.44 ± 0.02, $P < 0.01$) or 150 ppm bilobalide alone (0.57 ± 0.04, $P < 0.001$) significantly

Table 3
PCNA-labeling index in rectal section of colonic mucosa

Group no.	Treatment (no. of rats)	'Normal-appearing' crypts	Normal crypts
1	AOM alone (8)	27.0 ± 4.5[a] (10)	–
2	AOM + 50 ppm EGb (8)	18.4 ± 4.0[b] (10)	–
3	AOM + 500 ppm EGb (8)	9.6 ± 3.8[c] (10)	–
4	AOM + 15 ppm bilobalide (8)	16.2 ± 3.1[d] (10)	–
5	AOM + 150 ppm bilobalide (8)	15.2 ± 4.6[b] (10)	–
6	500 ppm EGb (4)	–	12.0 ± 1.8 (10)
7	150 ppm bilobalide (4)	–	11.3 ± 2.2 (10)
8	No treatment (4)	–	9.8 ± 3.2 (10)

AOM, azoxymethane; ACF, aberrant crypt foci. No. in parentheses of the data are no. of ACF or crypts examined.
[a] Mean ± SD.
[b] Significantly different from group 1 by Welch's t-test ($P < 0.01$).
[c] Significantly different from group 1 by Welch's t-test ($P < 0.001$).
[d] Significantly different from group 1 by Welch's t-test ($P < 0.005$).

Table 4
Measurement of drug metabolizing enzymes in liver

Group No.	1	2	3	4	5	6	7	8
	(AOM)	(AOM + EGB 50 ppm)	(AOM + EGb 500 ppm)	(AOM + bilobalide 15 ppm)	(AOM + bilobalide 150 ppm)	(EGb 500 ppm)	(bilobalide 150 ppm)	(none)
Cytochrome P450 (nmol/mg)	0.39 ± 0.04[a]	0.37 ± 0.04	0.58 ± 0.18	0.61 ± 0.09[b]	0.91 ± 0.20[c]	0.66 ± 0.05[d]	1.15 ± 0.13[d]	0.35 ± 0.08
Cytochrome b_5 (nmol/mg)	0.33 ± 0.03	0.37 ± 0.03	0.48 ± 0.03[e]	0.46 ± 0.02[e]	0.57 ± 0.09[b]	0.44 ± 0.02[f]	0.57 ± 0.04[d]	0.35 ± 0.04
NADPH- cytochrome P450 reductase (nmol/min/mg)	152 ± 8	179 ± 24	182 ± 17[c]	174 ± 17	216 ± 20[b]	173 ± 15	157 ± 29	149 ± 17
EROD (pmol/min/mg)	90 ± 15	118 ± 13[c]	230 ± 28[e]	206 ± 13[e]	237 ± 27[e]	163 ± 17[d]	150 ± 42[g]	75 ± 13
MROD (pmol/min/mg)	31.2 ± 4.6	34.1 ± 9.2	43.5 ± 16	35.9 ± 9.7	19.4 ± 9.5	36.3 ± 12	12.7 ± 7.6[f]	30.9 ± 4.7
PNPH (nmol/min/mg)	0.66 ± 0.06	0.60 ± 0.19	1.09 ± 0.23[c]	1.18 ± 0.18[b]	1.50 ± 0.25[h]	1.34 ± 0.16[g]	1.79 ± 0.30[i]	0.77 ± 0.30
6β-OH (nmol/min/mg)	1.58 ± 0.10[d]	0.76 ± 0.16[e]	0.97 ± 0.28[h]	0.59 ± 0.31[b]	3.07 ± 0.61[c]	1.26 ± 0.16[d]	2.66 ± 0.88[g]	0.48 ± 0.07

EROD, Ethoxyresorufin *O*-deethylase, CYP1A1; MROD, Methoxyresorufin O-demethylase, CYP1A2; PNPH, *p*-Nitrophenol 2-hydroxylase, CYP2E1; 6β-OH, Testosterone 6β-hydrpxylase, CYP3A.

[a] Mean ± SD.

[b] Significantly different from group 1 by Welch's *t*-test or Student's *t*-test ($P < 0.005$).

[c] Significantly different from group 1 by Welch's *t*-test or Student's *t*-test ($P < 0.05$).

[d] Significantly different from group 8 by Welch's *t*-test or Student's *t*-test ($P < 0.001$).

[e] Significantly different from group 1 by Welch's *t*-test or Student's *t*-test ($P < 0.001$).

[f] Significantly different from group 8 by Welch's *t*-test or Student's *t*-test ($P < 0.01$).

[g] Significantly different from group 8 by Welch's *t*-test or Student's *t*-test ($P < 0.05$).

[h] Significantly different from group 1 by Welch's *t*-test or Student's *t*-test ($P < 0.01$)

[i] Significantly different from group 8 by Welch's *t*-test or Student's *t*-test ($P < 0.005$).

increased the cytochrome b_5 content when compared to group 8 (0.35 ± 0.04). A significant increase in NADPH- cytochrome P450 reductase activity was detected in the groups 3 (182 ± 17, $P < 0.05$) and 5 (216 ± 20, $P < 0.005$). Dietary feeding of EGb or bilobalide also affected the activities of CYP (Table 4). CYP 1A1 elevated in groups 2 ($P < 0.05$), 3 ($P < 0.001$), 4 ($P < 0.001$), and 5 ($P < 0.001$) when compared to group 1. Feeding with EGb (500 ppm) and bilobalide (150 ppm) alone also increased CYP1A1 when compared to group 8 ($P < 0.001$ and $P < 0.05$, respectively). CYP 1A2 in rats given 150 ppm bilobalide alone was significantly higher than group 8 ($P < 0.01$). Treatment with AOM and 500 ppm EGb significantly increased CYP2E1 when compared to group 1 ($P < 0.05$). CYP2E1 activities in groups 4 and 5 were also higher than group 1 ($P < 0.005$ and $P < 0.01$, respectively.) The values of groups 6 and 7 were significantly greater than group 8 ($P < 0.05$ and $P < 0.005$, respectively). As for CYP3A, AOM exposure significantly elevated the activity when compared to group 8 ($P < 0.001$). The treatment with EGb or bilobalide at both doses together with AOM except for group 5 significantly lower this increase, although feeding with EGb (group 6) or bilobalide (group 7) increase liver CYP3A when compared with untreated rats (group 8)

3.5. Alterations in the activities of GST and QR

Feeding with the diet containing EGb or bilobalide alone resulted in a significant increase in hepatic GST (Fig 4A) and QR (Fig. 4B) activities when compared to untreated rats (group 8). A significant increase in GST was detected in the groups given feed containing bilobalide at the concentrations of 15 ppm (1.32 ± 0.04, $P < 0.005$) and 150 ppm (1.89 ± 0.17, $P < 0.001$) along with AOM injection compared to group 1 (AOM alone, 0.90 ± 0.11) (Fig. 4A). Liver QR activity in the group 5 (150 ppm bilobalide with AOM injection:

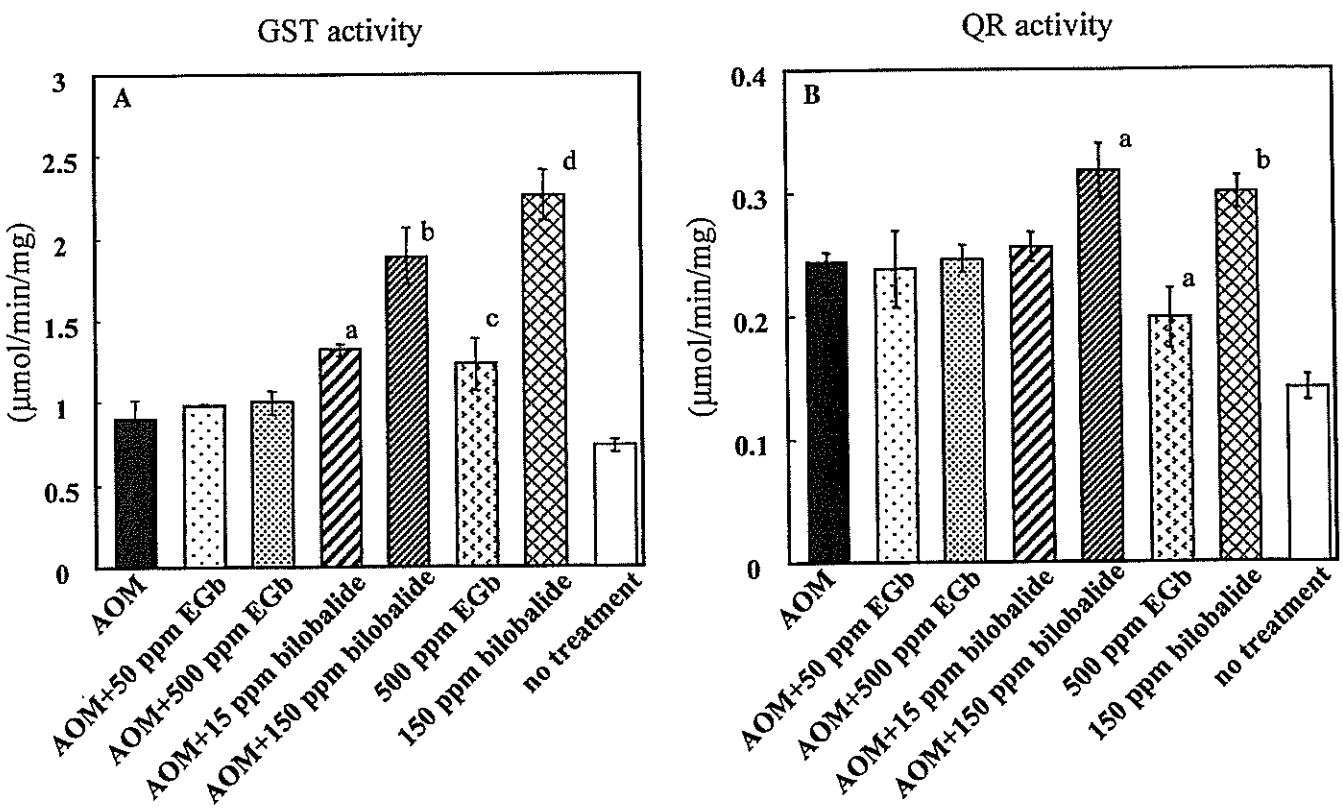

Fig. 4. Liver cytosolic GST and QR activities in rats treated with EGb or bilobalide. A, GST activity. a,b, Significantly different from group 1 (AOM alone) by Welch's t-test or Student's t-test ($^aP < 0.005$ and $^bP < 0.001$); c,d, Significantly different from group 8 (no treatment) by Welch's t-test or Student's t-test ($^cP < 0.01$ and $^dP < 0.001$) B, QR activity. a, Significantly different from group 1 (AOM alone) by Welch's t-test or Student's t-test ($^aP < 0.005$); b, Significantly different from group 8 (no treatment) by Welch's t-test or Student's t-test ($^bP < 0.001$).